Supersubstorms during strong magnetic storm on 7 September 2017

Irina Despirak[1*], *Natalia* Kleimenova[2], *Liudmila* Gromova[3], *Sergey* Gromov[3], and *Liudmila* Malysheva[2]

[1]Polar Geophysical Institute, Apatity, Russia
[2]Schmidt Institute of the Physics of the Earth RAS, Moscow, Russia
[3]Pushkov Institute of Terrestrial Magnetism, Ionosphere and Radio Wave Propagation, Troitsk, Moscow, Russia

Abstract. We analyzed the appearance of two supersubstorms observed during storm on September 07, 2017. Supersubstorms (SSS) are called substorms with SML index < - 2500 nT. The storm on September 07, 2017 is famous event which was studied already in many papers. There were two several geomagnetic storms on 7 and 8 September 2017, which associated with two consecutive solar wind structures: SHEATH with EJECTA and SHEATH with magnetic cloud (MC). Because the first SHEATH have a positive IMF Bz on their front edge the substorm activity absent in this time. The main phase of the first magnetic storm began with arriving the second SHEATH with the strong negative IMF Bz. During this period the first night-side supersubstorm (up to ~ 3500 nT) developed. The second magnetic storm was caused by MC with the negative IMF Bz and the severe night-side supersubstorm (up to ~ 3500 nT) were registered in this time. Thus, during the 7-8 September 2017 storms, two supersubstorms were generated, these supersubstorms caused by the SHEATH and MC impact have demonstrated the global scale distribution.

1. Introduction

The topic of our study is supersubstorms (SSS), which are very intense magnetic substorms. These extreme events generating considerable interest in terms of an understanding of the physical interaction processes in the solar wind - Earth's magnetosphere - ionosphere system. The investigation of SSS was began recently, the first paper about observations of these very strong substorms was work of Tsurutani et al. [1]. Since the studies were recently started, nothing is yet known about the relationship between earthquakes and supersubstorms. However, if we will find the precursors of earthquakes in geomagnetic disturbances, then we need to consider very intense geomagnetic disturbances, such as the supersubstorms.

Supersubstorms were called in [1] to designate very strong substorms. when the analysis of ground-based observations from the SuperMAG magnetometer network were carried. SSS are very intense magnetic substorms observed when the SML or AL indexes of geomagnetic activity reach very high negative values (< -2500 nT). The SML index is a generalization of the well-known AL index [2], but SML index was calculated by all stations of SuperMAG network. Therefore, it included not only 12 stations of the auroral zone in the Northern hemisphere (from ~ 60^0 to ~70^0 geomagnetic latitudes), which used usually for the determination of AL/AE indexes, but more another magnetic stations,

*Corresponding author: despirak@gmail.com

located on higher and lower latitudes. Thus, SML index reflects better the planetary activity during strong geomagnetic disturbances.

Great number of examples of the SSS observations may find in the previous works [1], [3] and [4], and therefore we not included the example of SSS in this paper. In works [1], [3], [4] questions about possible occurrence of such intense supersubstorms were considered. It is shown that SSS events can be observed during any phase of the solar cycle, but their highest frequency falls in the declining phase of the cycle and the lowest occurs during the cycle minimum [2]. But it is known that very intense magnetic storms, the so-called superstorms (Dst ≤ –250 nT), have been observed namely during the declining phase of solar activity. So, one could suppose that SSS events are observed namely during superstorms. However, it is shown that SSS events are not always associated with very intense storms and can be observed during less intense (−100 nT ≥ Dst > −250 nT) and moderate (−50 nT ≥ Dst > −100 nT) magnetic storms, and even during nonstorm (Dst > −50 nT) intervals [1], [4].

SSS events are detected during defined conditions in the solar wind, namely during the long-term southward interplanetary magnetic field, which is usually associated with solar wind magnetic clouds (MCs) or a SHEATH plasma compression region ahead of a MC ([1], [4]). Furthermore, most SSS events are associated with density jumps and pressure pulses in the solar wind. It was considered also the SSS distribution by types of the solar wind and was shown that SSS occurrence is associated with interplanetary manifestations of coronal mass ejections (CME) and, in fact, bears no relationship to high-speed streams from coronal holes [4].

It is known that solar wind is not inhomogeneous, there are different streams and structures [5], [6], [7]. The complex large-scale structures of the solar wind can be divided into three main types: (i) Slow solar wind. It is the slow flux of solar plasma above the coronal streamers, with the velocity ~ 300-450 km/s (ii) Quasistationary high speed streams over coronal holes (velocity ~600-1000 km/s). These streams responsible for recurrent geomagnetic disturbances. (iii) Interplanetary Coronal mass ejections (CME), which are sources of sporadic high-speed streams and sporadic geomagnetic activity. At the present time different classifications of the solar wind types were developed; one of these is the catalog of large-scale solar wind phenomena [8]. In our work we used this catalog for determination of solar wind types.

The aim of our work is the study of the substorm activity during storm 07-08 September 2017, namely the spatial behavior of two supersubstorms events observed during this storm. For this purpose, the data from the SuperMAG global magnetometer network and Scandinavian magnetometer profile IMAGE were used.

2. Data

Solar wind types were defined by the catalog of the large-scale solar wind phenomena (ftp://ftp.iki.rssi.ru/omni/) and by the OMNI data base. In this catalog there were 3 quasistationary, 5 disturbed types of the solar wind and shock waves are distinguished: 1) heliospheric current sheet (HCS); 2) slow plasma flows above streamers (SLOW); 3) high speed streams over polar coronal holes (FAST); 4) and 5) coronal mass ejections, which consists from body of CME – magnetic cloud (MC) or EJECTA- and the plasma compression region on their front (SHEATH); 6) a plasma compression region before the fast stream (CIR);7) and 8) direct and reverse shock waves (IS and Isa).

Extremely intense substorms (SSS) were determined by SML or AL indices, based on the data from magnetic ground-based observations of the SuperMAG network (http://supermag.jhuapl.edu/) and Scandinavian IMAGE network (http://space.fmi.fi/image/). Supersubstorms are defined as those events with peak SML < -2500 nT ([1], [3]). The latitudinal propagation of SSS we defined by equivalent currents distribution obtained

by MIRACLE system. The spatial distribution of SSS were determined by the SuperMAG network and the picture of electric field vectors obtained by SuperMAG network.

3. Results

In early September 2017, a series of solar flares and coronal mass ejections (CMEs) erupted from the Sun. Three solar flare were registered on 06-07 September 2017. Second flare was class X.9, and was recorded by STEREO-A spacecraft as the CME on 06 September 2017, which erupted from the southwest of the solar disk at 12:24 UT, the average speed of CME is estimated to be ≈1400 km/s [9]. The CME reached the Earth`s orbit on ~22-23 UT 07 September. This CME associated with magnetic storm on 7 -8 September 2017.

3.1. Interplanetary conditions

Solar wind and Interplanetary Magnetic Field (IMF) parameters for time period 06-09 September 2017 are presented in Figure 1. These parameters were taken from the 1-min sampled OMNI data base of the CDAWeb (http://cdaweb.gsfc.nasa.gov/cgi-bin/eval2.cgi). It is seen that two consecutive structures in the solar wind were observed: SHEATH with EJECTA and SHEATH with Magnetic Cloud (MC). The region SHEATHs are marked by green crosshatched area, EJECTA- by orange crosshatched area, Magnetic Cloud (MC) – by red crosshatched area. The shock waves (IS) are marked by vertical red lines.

There were two several geomagnetic storms on 7 and 8 September 2017, which associated with second structure (SHEATH+MC)**.** Because the first SHEATH have a positive IMF Bz on their front edge, it not caused the magnetic storm and the substorm activity absent in this time. The main phase of the first magnetic storm began with arriving the second SHEATH with the strong negative values of the IMF Bz. The second magnetic storm was caused by MC with the negative IMF Bz component. Against the background of these two storm development were registered two supersubstorm: the first night-side supersubstorm (SML index up to ~ 3500 nT) was observed during second SHEATH, and the second night-side supersubstorm (SML index was ~ 2500 nT) was registered during magnetic cloud.

3.2. Supersubstorm determination

In Fig.2 shown the variations of SML index from 16 UT on 7 September to 22 UT on 8 September 2017. Supersubstorms are defined as those events with peak SML < -2500 nT. It is seen that two supersubstorms were observed in this period: on 7 September at ~23:45 UT, which is marked as SSS-1 in Fig.2, and on 8 September at ~13:00 UT, which is marked as SSS-2. The SSS-1 was associated with the second SHEATH impact and the SSS-2 – with the MC impact. The SSS-1 intensity was stronger due to the higher values of IMF Bz.

In section 3.3 and 3.4 were considered the spatial distributions of the geomagnetic disturbances during these two supersubstorms by SuperMAG and IMAGE magnetometers network data.

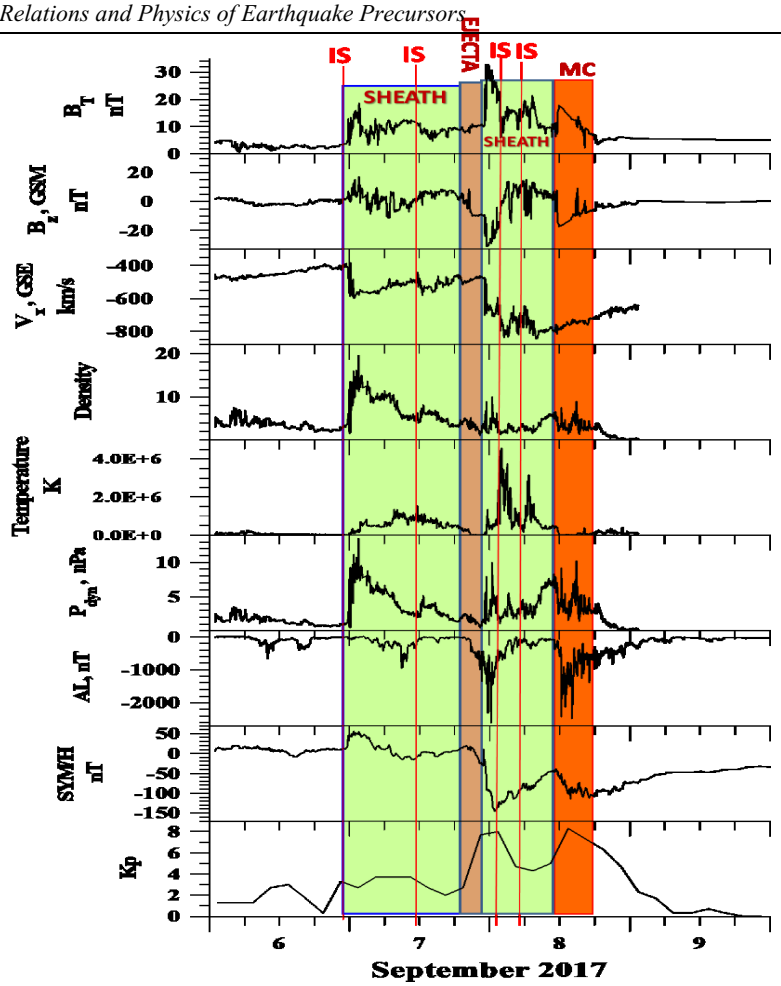

Fig. 1 Solar wind and interplanetary magnetic field parameters for the period 6-9 September 2017. From top to bottom: the Interplanetary Magnetic Field magnitude (B_T), the IMF Z-component (B_Z), the X-component of the velocity (V_X), the solar wind density (N), the temperature (T), the dynamic pressure (P), and the geomagnetic indices AL, SYMN/H and Kp.

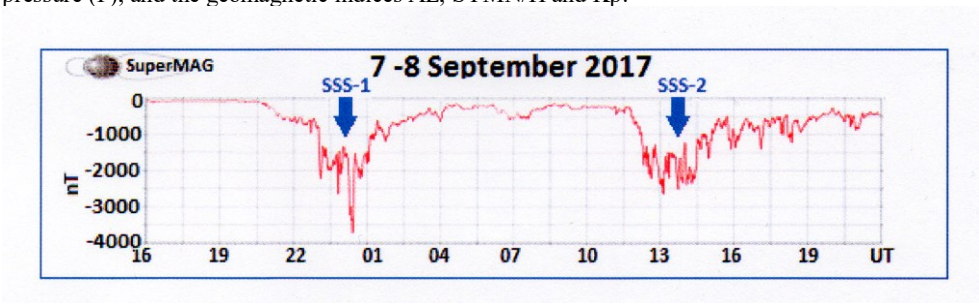

Fig.2. The behavior of SML index from 16 UT on 7 September to 22 UT on 8 September

3.3. First supersubstorm (SSS-1)

Fig.3 presents the spatial distribution of magnetic disturbances during first supersubstorm (SSS-1). It is seen that maximal disturbances were registered at auroral latitudes, at IMAGE meridian, in the post-midnight sector. Variations of X-component of magnetic field are shown at the top panels of Fig.3a. It is seen that the strong magnetic field variations (more ~1000 nT) were observed. The development of the westward electrojet during SSS-1 shown at the left picture (Fig 3b), where equivalent westward and eastward currents were

presented. It confirms that the development of supersubstorm was at the auroral latitudes, in the post-midnight sector. However, simultaneously were observed the bay-like magnetic disturbances located at the polar latitudes, at stations NAQ, BLC (morning sector), BRW (near noon) (Fig 3a, bottom panels). The SuperMAG map of the electric field vectors (Fig. 3c) shows that the westward electrojet was developed in the global scale, reaching the day side region.

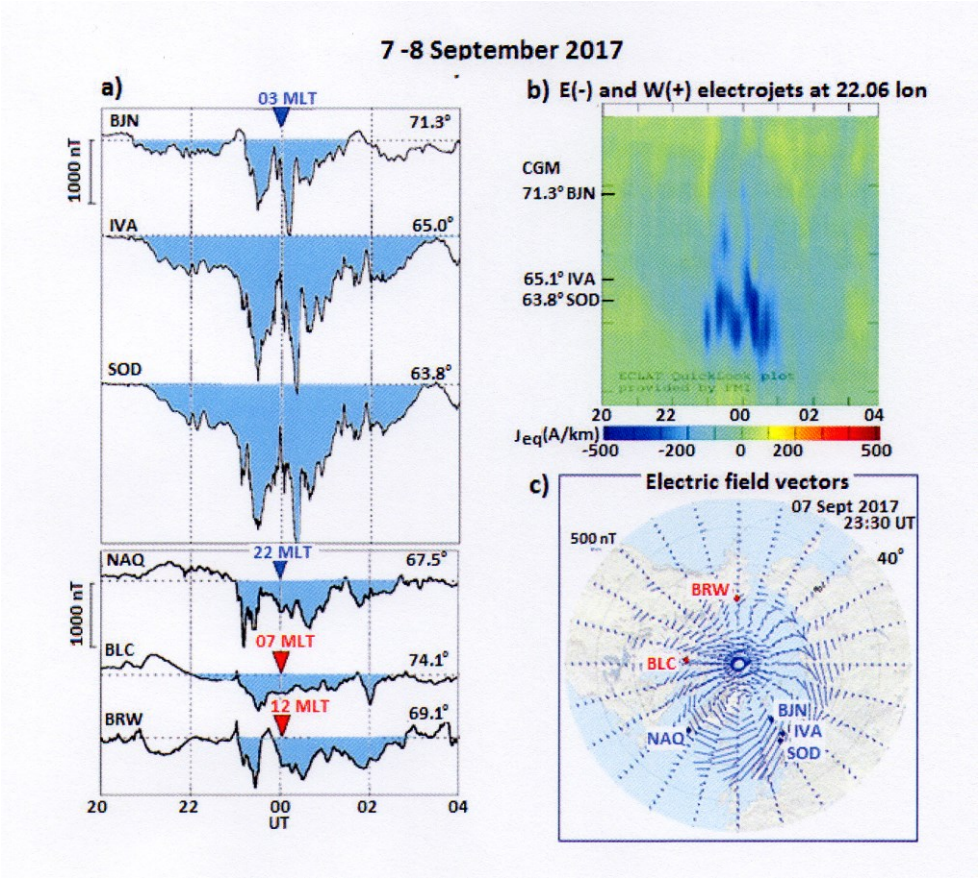

Fig. 3. Spatial distributions of disturbances during SSS-1: a) Variations of X-component of magnetic field at auroral stations BJN, IVA, SOD (top) and at polar stations NAQ, BLC, BRW (bottom); b) picture of equivalent currents development by MIRACLE system; c) picture of electric field vectors development obtained from SuperMag network

3.4. Second supersubstorm (SSS-2)

Fig.4 presents the spatial distribution of magnetic disturbances during second supersubstorm (SSS-2). It is seen that maximal disturbances were registered also at auroral latitudes, in the post-midnight sector. Noted that magnetic stations of American sector (BRW, CMO, YKC) located in the post-midnight sector in this time (Fig 4a, top panels) and the strong magnetic field variations (more ~1000 nT) were observed here. Simultaneously were observed the bay-like magnetic disturbances at stations of IMAGE network, which located in the noon sector in this time (NAL, BJN and SOR). It is seen that these disturbances were focused only at the polar latitudes (Fig 4a, bottom panels). The picture of equivalent currents development (Fig. 4b) confirms this. The SuperMAG map of

the electric field vectors (Fig. 4c) shows that the westward electrojet was developed in the global scale, from the post-midnight sector to noon sector.

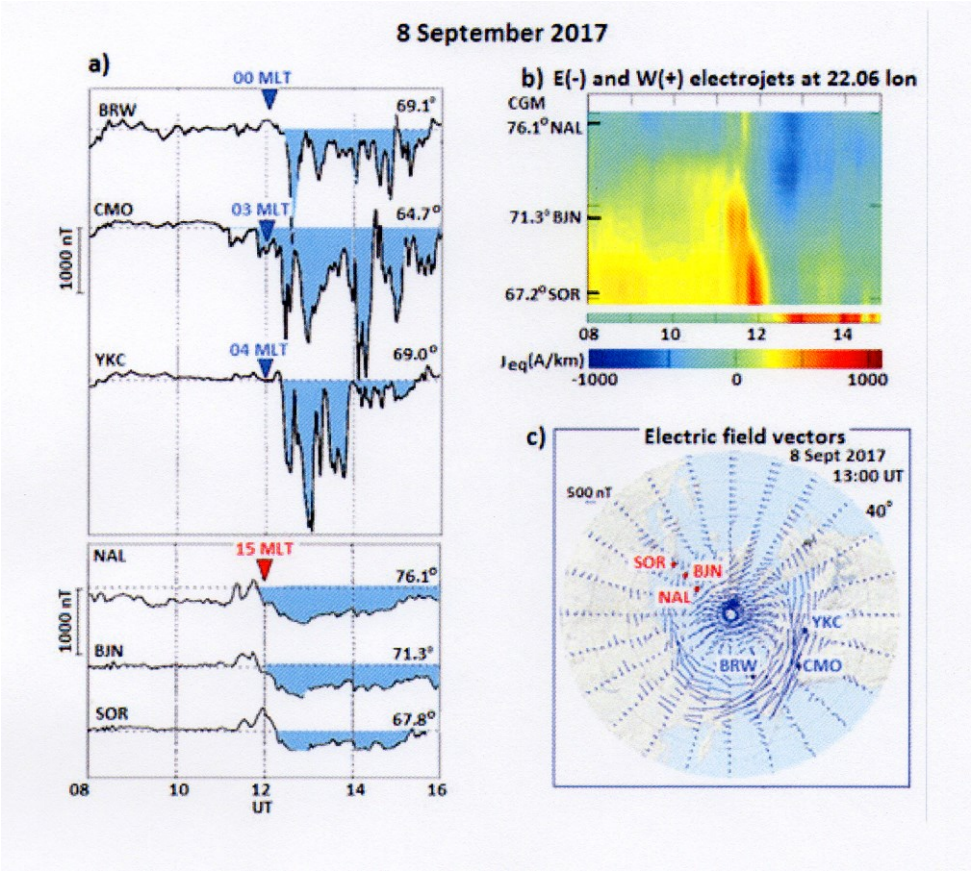

Fig. 4. Spatial distributions of disturbances during SSS-2: a) Variations of X-component of magnetic field at auroral stations BRW, CMO, YKC (top) and at polar stations NAL, BJN, SOR (bottom); b) picture of equivalent currents development obtained from MIRACLE system; c) picture of electric field vectors development obtained from SuperMag network

4. Discussion

The SSS-1 was associated with the second SHEATH impact and the SSS-2 – with the MC impact. The SSS-1 intensity was stronger due to the higher values of IMF Bz. The strongest magnitude of both SSSs was observed at the post-midnight auroral latitudes and was accompanied by the bay-like disturbances at day-side polar latitudes with significantly reduced intensity. The maps of the vectors of SuperMAG electric field demonstrate that the ionospheric currents were recorded in the global scale around the Earth.

5. Conclusions

1) Two suppersubstorms, i.e. very intense substorms [1}; [3]; [4], have been observed during the strong magnetic storm on 7-8 September 2017.

2) For the first time, it was found that suppersubstorms could develop in the global scale surrounding the Earth.

6. References

1. B.T. Tsurutani, R. Hajra, E. Echer, J.W. Gjerloev, Ann. Geophys. **33**, 519–524, (2015).
2. T.N. Davis, M. Sugiura, J. Geophys. Res., **71**, 785–801, (1966), doi 10.1029/ JZ07li003p00785
3. R. Hajra, B.T. Tsurutani, E. Echer, W.D. Gonzalez., J.W. Gjerloev. J. Geophys. Res., **121**, 7805–7816, (2016), doi: 10.1002/ 2015JA021835.
4. I.V. Despirak, A.A. Lyubchich, N.G. Kleimenova. Geomagn. Aeron., **59**, no. 2, 170, (2019)
5. M.I. Pudovkin, M.I. Sorovskii Obraz. Zh. **12**, 87–94, (1996).
6. Yu. I. Yermolaev, Planet. Space Sci., **39**, no. 10, 1351–1361, (1991).
7. K. Liou, T. Sotirelis., I. Richardson. J. Geophys. Res. **123**. 485–496, (2018), doi:10.1002/2017JA02445
8. Yu.I. Yermolaev, N.S. Nikolaeva, I.G. Lodkina, M.Yu. Yermolaev, Cosmic Research (Engl. Transl.), **47**, 81-94, (2009).
9. C.-C. Wu, K. Liou, R.P. Lepping, L. Huttuning, Solar Phys., **294**, (2019), doi.org/10.1007/s11207-019-1446-2.